Tendon and Motor Phenotypes in the *Crtap*$^{-/-}$ Mouse Model of Recessive Osteogenesis Imperfecta

Matthew W. Grol[1], Nele A. Haelterman[1], Elda M. Munivez[1], Marilyn Archer[2], David Hudson[2], Sara F. Tufa[3], Douglas R. Keene[3], David Eyre[2] and Brendan H. Lee[1†]

[1] Department of Molecular and Human Genetics, Baylor College of Medicine, Houston, TX

[2] Department of Orthopaedics and Sports Medicine, University of Washington, Seattle, WA

[3] Shriners Hospital for Children, Portland, OR

[†] Correspondence and reprint requests:

Brendan H. Lee, MD, PhD

Department of Human and Molecular Genetics

One Baylor Plaza, ABBR-R814

Baylor College of Medicine

Houston, TX 77030

Email: blee@bcm.edu

Tel: +1 713-798-7246

Fax: +1 713-798-4523

Running Title: Tendon and motor deficits in Osteogenesis Imperfecta

Keywords: osteogenesis imperfecta, tendon, ligament, cross-link, motor behavior

ABSTRACT

Osteogenesis imperfecta (OI) is a heterogeneous group of connective tissue disorders characterized by variable short stature, skeletal deformities, low bone mass with increased bone fragility, and motor deficits. The majority of cases are caused by mutations in type I collagen, or by mutations that affect collagen processing and/or modification. Like bone, the extracellular matrix of tendons and ligaments is largely made up of type I collagen; however, despite the fact that a subset of OI patients presents with joint hypermobility, how tendon/ligament dysfunction contributes to this is unknown. Here, we performed a detailed phenotypic characterization of the flexor digitorum longus (FDL) tendon, Achilles tendon and patellar ligament in the *Crtap* mutant mouse model of severe, recessive OI. Stable, pyridinoline collagen cross-links were increased by 5- to 10-fold in mutant tendons and ligaments. Collagen fibril size in all three structures was also smaller in *Crtap*$^{-/-}$ mice compared to wildtype or heterozygous littermates. Together, these ultrastructural and biochemical changes resulted in thinner tendons and ligaments with increased cellularity compared to controls, as assessed by histology. To examine how alterations in tendons might affect motor function, we performed a battery of behavioral assays. During open field assessment, *Crtap*$^{-/-}$ mice exhibited reduced horizontal and vertical activity. *Crtap*$^{-/-}$ mice also exhibited motor impairments on the rotarod and grid footslip tests. In addition, *Crtap*$^{-/-}$ mice had reduced grip strength and displayed reduced time on the inverted grid test, indicating that they are weaker than wildtype and heterozygous mice. In summary, these data demonstrate that the tendons/ligaments of *Crtap*$^{-/-}$ mice are pathologically altered compared to wildtype – a phenotype that correlates with motor deficits and grip strength impairments. As such, *Crtap*$^{-/-}$ mice provide a preclinical model with which to examine downstream mechanisms and therapies pertaining to tendon/ligament pathology and motor dysfunction for OI patients.

INTRODUCTION

Tendon is a fibrous tissue that connects skeletal muscle to bone to facilitate motion, whereas ligaments connect articulating bones to support joint alignment and function[1, 2]. The extracellular matrix of tendons and ligaments is primarily composed of type I collagen as well as smaller quantities of other collagens and proteoglycans[3]. During development, the collagen fibrils in tendons and ligaments develop through addition and lengthening before transitioning to appositional fusion of existing fibers with continued lengthening in post-natal life[4]. The synthesis and assembly of this collagen-rich matrix is influenced by other small collagens and proteoglycans as well as by the cross-linking chemistry of type I procollagen fibrils, which in turn regulates fibril size and strength[5]. Like tendon and ligament, the organic matrix of bone consists largely of type I collagen[6], and disruptions in collagen synthesis and folding have been shown to negatively impact its biochemical and mechanical properties in connective tissue diseases such as Osteogenesis Imperfecta (OI)[7]. However, despite evidence of joint mobility phenotypes and motor deficits in OI patients[8, 9], tendon and ligament phenotypes in this disease are relatively understudied.

OI is a heterogeneous group of disorders characterized by variable short stature, skeletal deformities, low bone mass, and increased bone fragility. Approximately 80% of OI cases are caused by dominantly inherited mutations in the genes encoding the $\alpha1$(I) or $\alpha2$(I) chains of type I collagen. Mutations in genes responsible for the synthesis, post-translational modification and processing of collagen, such as cartilage-associated protein (CRTAP), lead to severe, recessive forms of this disease[7]. In addition to skeletal defects, other connective tissue manifestations including joint hypermobility and skin hyperlaxity are observed in a subset of OI patients[8, 9]. Our and others' studies have shown that CRTAP forms a complex with Prolyl 3-

70 hydroxylase 1 (P3h1, encoded by *Lepre1*) and Cyclophilin B (CypB, encoded by *Ppib*), and is
71 required for prolyl 3-hydroxylation of type I procollagen at Pro986 of chain α1(I) and Pro707 of
72 chain α2(I)[10-12]. In this regard, loss of either CRTAP or P3H1 leads to loss of this complex and
73 its activity, causing a severe recessive form of OI characterized by short stature and brittle
74 bones[11, 13-15]. Collagen isolated from *Crtap*$^{-/-}$ and *Lepre1*$^{-/-}$ mice is characterized by lysine over-
75 modifications and abnormal fibril diameter[11, 14]. A comprehensive analysis of *Crtap*$^{-/-}$ mice has
76 revealed multiple connective tissue abnormalities, including in lungs, kidneys, and skin[16];
77 however, the impact of loss of Crtap on tendons and ligaments remains unknown.
78 Alterations in collagen fibril size and cross-linking have been noted in a limited number
79 of studies using dominant or recessive mouse models of OI[17-19]; however, whether loss of Crtap
80 impacts tendon and ligament development and structure remains unknown. In this study, we
81 show that *Crtap*$^{-/-}$ mice have thinner Achilles tendons and patellar ligaments at 1 and 4 months-
82 of-age that are hypercellular with a reduction in total ligament volume. Moreover, the patellar
83 and cruciate ligaments from *Crtap*$^{-/-}$ show increased cell size and variable ectopic
84 chondrogenesis by 4 months-of-age. Examining the collagen matrix, we found an increase in
85 stable (irreversible) collagen cross-links at both timepoints, accompanied by alterations in fibril
86 diameter at 4-months compared to wildtype controls. These changes in the tendons and ligaments
87 of *Crtap*$^{-/-}$ mice were accompanied by motor deficits and reduced strength at 4 months-of-age. In
88 conclusion, loss of Crtap in mice causes a tendinopathy-like phenotype and significant
89 behavioral impairments.
90

91 **MATERIALS AND METHODS**

92 *Animals*

93 *Crtap*$^{-/-}$ mice were generated as previously described[11] and maintained on a mixed C57BL/6J
94 and 129Sv genetic background. All studies were performed with approval from the Institutional
95 Animal Care and Use Committee (IACUC) at Baylor College of Medicine. Mice were housed 3
96 to 4 mice to a cage in a pathogen-free environment with *ad libitum* access to food and water and
97 under a 14h light/10h dark cycle.
98
99 *Histological analysis*
100 Mice were euthanized and ankle and knee joints were dissected and fixed for 48 h on a shaker at
101 room temperature in freshly prepared 4% paraformaldehyde (PFA) in 1× phosphate-buffered
102 saline (PBS). Samples were decalcified at 4°C using 10% ethylenediaminetetraacetic acid
103 (EDTA) in 1×PBS for 10 days (with one change out at 5 days) prior to paraffin embedding using
104 a standard protocol. Samples were sectioned at 6 μm and stained with hematoxylin and eosin
105 (H&E) to visualize tendon structures.
106
107 *Phase-contrast μCT imaging and analysis*
108 To quantify tendon/ligament volume, knee joints were dissected from mice, stained with contrast
109 agents, scanned by phase-contrast μCT, and analyzed using TriBON software (RATOC, Tokyo,
110 Japan) as previously described for articular cartilage[20-23]. In addition to the articular surfaces
111 (data not shown), we performed contrast-enhanced visualization of the patellar ligament using
112 this protocol. To quantify volume, samples were examined in transverse where the patellar
113 ligament boundary was easily distinguished from the joint capsule. Ligament volume was
114 assessed from its origin within the patella to its insertion at the tibia.
115

116 *Transmission electron microscopy analysis of collagen fibril size*

117 Mouse ankle and knee joints were dissected and fixed in fresh 1.5% glutaraldehyde/1.5% PFA
118 (Tousimis) with 0.05% tannic acid (Sigma) in 1×PBS at 4°C overnight to preserve the native
119 tension on relevant tendons/ligaments. The next day, flexor digitorum longus (FDL) and Achilles
120 tendons as well as patellar ligament were dissected out in 1×PBS, and placed back into fixative.
121 Samples were then post-fixed in 1% osmium tetroxide (OsO_4), rinsed in Dulbecco's Modified
122 Eagle Medium (DMEM) and dehydrated in a graded series of ethanol to 100%. Samples were
123 rinsed in propylene oxide, infiltrated in Spurrs epoxy, and polymerized at 70°C overnight. TEM
124 images were acquired using a FEI G20 TEM at multiple magnifications to visualize transverse
125 sections of collagen fibrils. Collagen fibril diameter was measured using the Fiji release of
126 ImageJ[24].

127

128 *Tendon collagen cross-linking analysis*

129 Collagen hydroxylysyl-pyridinoline (HP) cross-links were quantified as previously described[25,
130 26]. In brief, tendons and ligaments isolated from hindlimbs were hydrolyzed by 6M HCl for 24h
131 at 108°C. Dried samples were then dissolved in 1% (v/v) n-heptafluorobutyric acid for
132 quantitation of HP by reverse-phase HPLC with fluorescence monitoring.

133

134 *Open field assessment of spontaneous motor activity*

135 Open field activity was measured using the VersaMax Animal Activity Monitoring System
136 (AccuScan Instruments, Columbus, OH). On the day of assessment, mice were transferred to the
137 test room and allowed to acclimate in their home cage for 30 min at 50 Lux of illumination with
138 60 dB of white noise. Mice were then placed individually into clear 40 cm × 40 cm × 30 cm

139 chambers and allowed to move freely for 30 min. Locomotion parameters and zones were
140 recorded using the VersaMax activity monitoring software. Chambers were cleaned with 30-50%
141 ethanol to remove the scent of previously tested mice between each run.
142
143 *Rotarod analysis of motor coordination and endurance*
144 On the day of assessment, mice were transferred to the test room and allowed to acclimate within
145 their home cage for 30 min at 50 Lux of illumination with 60 dB of white noise. Mice were then
146 placed on a rotarod (UGO Basile, Varese, Italy) set to accelerate from 5-to-40 RPM over 5 min.
147 Five trials were performed per day for 2 consecutive days (trials 1-10) with a rest time of 5 min
148 between trials. Latency to fall was recorded when the mouse fell from the rotating rod or went
149 for two revolutions without regaining control. The rotarod was cleaned with 30-50% ethanol
150 between mice to remove the scent of previously tested animals.
151
152 *Grid footslip analysis of motor coordination*
153 The grid footslip assay consisted of a wire grid set atop a stand where movement was recorded
154 by a suspended digital camera. Mice were transferred to the test room on the day of assessment,
155 and allowed to acclimate within their home cage for 30 min at 50 Lux of illumination with 60 dB
156 of white noise. Mice were then placed one at a time on the grid and allowed to move freely for 5
157 min. The observer sat 6-8 feet away at eye-level to the mouse and recorded forelimb and
158 hindlimb footslips using the ANY-maze video tracking software (Stoelting Co., Wood Dale, IL).
159 At the completion of the test, mice were removed to their original home cage. Forelimb and
160 hindlimb footslips were normalized to the total distance traveled during the test.
161

Inverted grid analysis of strength and endurance

On the day of assessment, mice were transferred to the test room and allowed to acclimate within their home cage for 30 min at 50 Lux of illumination with 60 dB of white noise. Mice were then placed in the middle of a wire grid, held approximately 18-in above a cushioned pad and inverted. The latency to fall for each mouse was recorded. At the completion, mice were returned to their home cage.

Grip strength analysis

Mice were transferred to the test room on the day of assessment, and allowed to acclimate within their home cage for 30 min at 50 Lux of illumination with 60 dB of white noise. Each mouse was then lifted by its tail onto the bar of a digital grip strength meter (Columbus Instruments, Columbus, OH). Once both forepaws had gripped the bar, the mouse was pulled away from the meter by its tail with a constant speed until the forepaws released. The grip (in N of force) was recorded and the procedure repeated twice for a total of three measurements, which were averaged for the final result.

Statistical analysis

Data are presented as means ± S.D. or min-to-max box and whisker plots with individual data points. In the case of normal distribution, groups were compared using one-way ANOVA followed by Tukey's post-hoc tests. For non-normal distribution, groups were compared using Kruskal-Wallis followed by Dunn's post-hoc tests. For the Rotarod assay where time was a variable, groups were compared using two-way ANOVA followed by Bonferroni's post-hoc tests. Statistical analysis was performed using Prism 8.3.1 (GraphPad Software, La Jolla, CA).

185 For all tests, a *p*-value of < 0.05 was considered statistically significant.

186

187 **RESULTS**

188 *Crtap$^{-/-}$ mice exhibit abnormal tendon development*

189 Mice lacking Crtap present with growth delay, rhizomelia, and severe osteoporosis together with
190 disruption of other connective tissues including lung and skin[11, 16]. To assess whether *Crtap$^{-/-}$*
191 mice exhibit disruptions in the development of tendons and ligaments, we harvested ankle and
192 knee joints at 1 and 4 months-of-age to histologically examine the Achilles tendon and patellar
193 ligament. At 1-month, *Crtap$^{-/-}$* mice presented with thinner Achilles tendons and patellar
194 ligaments (**Figure 1C,F**) with increased cell numbers in both structures compared to wildtype
195 (**Figure 1A,D**) and heterozygous mice (**Figure 1B,E**). There was also a prominent hyperplasia of
196 the synovial membrane in *Crtap* mutant knees at this age (**Figure 1F**). By 4 months-of-age,
197 *Crtap$^{-/-}$* Achilles tendons and patellar ligaments remained thinner and hypercellular compared to
198 wildtype and heterozygous mice (**Figure 1G-L**); in addition, synovial hyperplasia persisted
199 within *Crtap$^{-/-}$* knees (**Figure 1L**). Interestingly, ectopic chondrogenesis was present towards
200 either end of the patellar ligament and/or cruciate ligaments in some (but not all) 4-month-old
201 *Crtap$^{-/-}$* mice (**Figure 1L**) – a phenomenon that can occur in tendinopathy[27].

202 To more accurately quantify the differences in tendon/ligament size between genotypes,
203 we employed phase-contrast μCT to examine differences in patellar ligament volume between
204 genotypes (**Figure 1M,N**) – a technique we previously used to examine soft tissues including
205 articular cartilage in intact murine knee joints[20-23]. In 4-month-old mice, we observed a thinning
206 of the patellar ligament compared to wildtype mice, with no notable changes in articular cartilage
207 surface (**Figure 1M**). Quantification revealed a decrease in patellar ligament volume in *Crtap$^{-/-}$*

208 but not heterozygous mice compared to wildtype controls (**Figure 1N**). Taken together, these
209 histological and μCT data demonstrate that *Crtap*$^{-/-}$ mice display disruptions in the development
210 and postnatal maturation of tendons and ligaments.
211
212 *Collagen fibril formation is altered in heterozygous and Crtap*$^{-/-}$ *mice*
213 Tendons develop embryonically via increased fibril length and number, whereas postnatal
214 growth arises from an increase in fibril length and diameter – the latter of which is driven by
215 lateral fusion of smaller fibrils[4]. To investigate the role of Crtap in collagen fibril maturation, we
216 utilized transmission electron microscopy (TEM) to examine changes in fibril diameter in flexor
217 digitorum longus (FDL) and Achilles tendons as well as patellar ligaments (**Figure 2**). In the
218 FDL tendon, there was a marked increase in small collagen fibrils (20-60 nm in size), a reduction
219 in 80-320 nm fibrils, and a slight increase in larger fibrils (>340 nm in diameter) in *Crtap*$^{-/-}$ mice
220 compared to wildtype (**Figure 2A,C,D**). Despite similarities seen in histology, heterozygous
221 mutant FDL tendons also exhibited a slight increase in 20-40 nm fibrils in mice compared to
222 wildtype controls (**Figure 2A-B,D**). Similar trends were observed for the Achilles tendon,
223 namely an increase in small fibrils (20-60 nm), a reduction in 80-240 nm fibrils and an increase
224 in large fibrils (> 280 nm) upon loss of *Crtap* (**Figure 2E,G-H**). In contrast to what we observed
225 for the FDL, heterozygous *Crtap*$^{-/+}$ Achilles tendons did not have increased numbers of smaller
226 fibers (**Figure 2F,H**). Instead, a greater number of fibrils ranging from 140-200 nm in size was
227 noted compared to wildtype controls.
228 Compared to the FDL and Achilles tendons, the greatest differences were seen within the
229 patellar ligament, though the pattern of changes remained consistent (**Figure 2I-L**). Specifically,
230 we observed a dramatic increase in 20 nm collagen fibrils compared to both heterozygous and

231 wildtype mice (**Figure 2I-L**). Fibrils ranging from 100-180 nm in diameter were reduced in
232 heterozygous and *Crtap*$^{-/-}$ mice compared to wildtype. Interestingly, the greatest difference from
233 wildtype was an increase in large collagen fibrils (>200 nm) in both heterozygous and *Crtap*$^{-/-}$
234 mice (**Figure 2I-L**). Taken together, these data indicate that heterozygosity and complete loss of
235 Crtap alters collagen fibril assembly in tendons and ligaments. In addition, the degree to which
236 collagen assembly is affected is site-dependent.
237
238 *Collagen cross-linking is increased in heterozygous and Crtap*$^{-/-}$ *mice*
239 Along with P3H1 and CyPB, CRTAP is an integral part of the collagen prolyl 3-hydroxylation
240 complex that is responsible for 3-hydroxylation of Pro986 of the type I procollagen α1 chain[7].
241 Loss of this complex blocks 3-hydroxyproline formation and affects lysine hydroxylation and
242 cross-linking in bone collagen[11, 12]; however, whether *Crtap*$^{-/-}$ mice exhibit altered collagen
243 cross-linking in tendon is unknown. To investigate this, we harvested tendons and ligaments at 1-
244 and 4-months and assessed for collagen cross-linking by quantifying the levels of hydroxylysyl-
245 pyridinoline (HP) (**Figure 3**). Overall, we observed an increase in these stable, mature collagen
246 cross-links from 1 to 4 months-of-age in all genotypes for the FDL and Achilles tendons (**Figure**
247 **3A-B**). In contrast, for the patellar ligament, age-dependent increases in collagen cross-links
248 were only observed in *Crtap*$^{-/-}$ mice (**Figure 3C**). For FDL tendons, *Crtap*$^{-/-}$ mice had more of
249 these collagen cross-links at 1- and 4-months compared to heterozygous and wildtype mice;
250 however, the content of HP residues per collagen decreased with age in this tissue (**Figure 3A**).
251 Interestingly, in Achilles tendons, an increase in collagen cross-linking was observed in both
252 heterozygous and *Crtap*$^{-/-}$ mice at 1-month compared to wildtype. In contrast, at 4-months, only
253 *Crtap*$^{-/-}$ mice had elevated collagen cross-links, and these levels were greater than those observed

254 at the earlier timepoint (**Figure 3B**).

255 Of the tissues examined, the patellar ligament showed the greatest increase in collagen
256 cross-links both with time and across genotypes. Specifically, collagen cross-links were elevated
257 by 5- to 10-fold in *Crtap*$^{-/-}$ patellar ligaments compared to heterozygous and wildtype at 1- and
258 4-months, respectively (**Figure 3C**). Taken together, these data suggest that *Crtap* is required for
259 proper hydroxylation and cross-linking of collagen fibrils in tendons and ligaments in a semi-
260 dominant fashion, as heterozygous mutant tendons/ligaments display a phenotype that is milder
261 than the phenotype observed for homozygous mutant mice. Importantly, the chemical quality of
262 collagen cross-linking appears to be spatiotemporally regulated and this regulation is
263 differentially affected by loss of a single or both copies of *Crtap*.

264

265 *Loss of CRTAP leads to deficiencies in motor activity, coordination and strength*

266 To investigate whether the tendon phenotypes observed in *Crtap*$^{-/-}$ have functional consequences,
267 we performed a series of behavioral assays at 4 months-of-age. Using the open field assay to
268 quantify changes in spontaneous motor activity, we observed that *Crtap*$^{-/-}$ mice displayed
269 significant reductions in both horizontal and vertical activity compared to heterozygous and
270 wildtype mice (**Figure 4A-B**). We next examined changes in motor coordination and endurance
271 using the rotarod assay. While no genotype-dependent differences were observed during the
272 learning phase of the assessment (Trials 1-5), *Crtap*$^{-/-}$ displayed a reduction in latency to fall for
273 Trials 6, 9-10 compared to wildtype and Trials 6, 8-10 compared to heterozygous mice (**Figure**
274 **4C**). To confirm this observation, we evaluated the mice using the grid footslip assay – an
275 alternative metric for motor coordination. In this regard, we found that *Crtap*$^{-/-}$ mice exhibited a
276 modest increase in forelimb and hindlimb footslips compared to heterozygous and wildtype mice

277 (**Figure 4D-E**). Taken together, these findings indicate that *Crtap*$^{-/-}$ mice have deficiencies in
278 motor activity and coordination compared to controls.
279 We next evaluated strength in the *Crtap*$^{-/-}$ mice using the inverted grid and grip strength
280 assays. Interestingly, we observed a decrease in the latency to fall during the inverted grid assay
281 for *Crtap*$^{-/-}$ mice compared to heterozygous and wildtype controls (**Figure 4F**). Using a more
282 quantitative metric, we examined these mice using the grip strength test and found that while
283 wildtype and heterozygous mice could generate approximately 1.3 N of force, mice lacking
284 CRTAP were weaker with a mean grip strength of 0.62 N (**Figure 4G**). Thus, *Crtap*$^{-/-}$ mice
285 display significant reductions in strength together with perturbations in motor activity and
286 coordination – behavioral changes that could be related in-part to their tendon phenotype.
287

288 **DISCUSSION**

289 In this study, we examined the histological, ultrastructural and biochemical characteristics of
290 tendons and ligaments in the *Crtap*$^{-/-}$ mouse model of severe, recessive OI. We demonstrate that
291 at 1- and 4 months-of-age, *Crtap*$^{-/-}$ have thinner, more cellular Achilles tendons and patellar
292 ligaments compared to heterozygous and wildtype mice. Using phase-contrast μCT imaging, we
293 confirmed that *Crtap*$^{-/-}$ patellar ligaments at 4-months are smaller than those from heterozygous
294 and wildtype mice. Examining collagen fibril organization, we found a marked alteration in
295 small and large fibrils in both heterozygous and *Crtap*$^{-/-}$ mice compared to wildtype that varied in
296 severity depending on the tendon or ligament being examined. Stable, HP cross-links were also
297 elevated at 1- and 4-months in *Crtap*$^{-/-}$ mice compared to wildtype, which indicates an increase
298 in telopeptide lysine hydroxylation and resulting irreversible intermolecular cross-links (see
299 below). Finally, we demonstrate that *Crtap*$^{-/-}$ mice exhibit motor impairments concomitant with

300 reductions in grip strength – a phenomenon that may be related to the tendon pathology observed
301 in these mice.

302 While collagen ultrastructure and cross-linking has been documented in mouse models of
303 dominant and recessive OI, there has been only modest histological characterization of tendons
304 and ligaments in these models. In this regard, we demonstrate that *Crtap*$^{-/-}$ mice have thinner
305 Achilles tendons and patellar ligaments at 1- and 4-months. Despite the reduction in size and
306 extracellular matrix, tendons and ligaments from these mice are hypercellular compared to
307 wildtype and heterozygous animals. While the alterations in tendon and ligament size and
308 cellularity may be a result of alterations in the collagen extracellular matrix, it could also be
309 associated with alterations in cellular signaling. In this regard, transforming growth factor beta
310 (TGF-β) signaling is upregulated in bones from *Crtap*$^{-/-}$ mice[28], and elevated TGF-β signaling
311 has been noted in mouse models with increased tendon cellularity and alterations in collagen
312 fibril distribution[29]. Further research is needed to elucidate the mechanisms that contribute to the
313 histological features noted within both tendons and ligaments in these mice.

314 Collagen fibril assembly is a dynamic process that begins with the formation of many
315 small fibrils that grow longitudinally during development, followed by appositional fusion and
316 continued longitudinal growth as tendons mature[4]. In the present study, we found an increased
317 proportion of small and large collagen fibrils in the FDL and Achilles tendons as well as patellar
318 ligaments of *Crtap*$^{-/-}$ mice compared to wildtype. These distributions varied in severity across the
319 three tissues, with the greatest differences being observed in the patellar ligament. *Lepre1*$^{-/-}$ mice
320 have been reported to display an increased proportion of small collagen fibrils in tail tendons[19],
321 indicating that loss of the 3-prolyl hydroxylase complex alters collagen fibrillogenesis. At the
322 same time, the increased number of small fibers was more pronounced in *Lepre1*$^{-/-}$ mice, and

323 there was no evidence of an increased proportion of large fibers[19] as observed for *Crtap*$^{-/-}$ mice in
324 this study. Similar to the *Lepre1*$^{-/-}$ mouse model, mice lacking CypB also exhibit a pronounced
325 increase in small collagen fibrils alone within tail tendons[18]. Together, this suggests that despite
326 forming a complex with P3h1 and CypB, loss of Crtap has distinct consequences on collagen
327 fibrillogenesis. In this regard, it is important to note that tail tendons were used for collagen fibril
328 distribution assessments in both *Lepre1*$^{-/-}$ and *Ppib*$^{-/-}$ mice[18, 19], whereas appendicular tendons
329 and ligaments were examined in our study. The difference in tissue type examined might also
330 explain why we observed unique alterations in collagen fibril distribution in heterozygous *Crtap*
331 mice, whereas *CypB* heterozygous tendons were indistinguishable from wildtype[18].
332 Type I procollagen molecules undergo post-translational modifications within the
333 endoplasmic reticulum, including lysyl-hydroxylation and prolyl-hydroxylation, that are critical
334 for proper collagen synthesis, transport and stability. Specifically, telopeptide lysine
335 hydroxylation results in mature lysyl-pyridinoline (LP) or hydroxylysyl-pyridinoline (HP)
336 residues after lysyl oxidase oxidation, which as permanent, irreversible crosslinks play a role in
337 regulating fibril growth and strength[25, 30]. Previous literature has demonstrated that loss of the 3-
338 prolyl hydroxylase complex caused by deletion of P3h1 (*Lepre1*$^{-/-}$) or Crtap (*Crtap*$^{-/-}$) prevents
339 prolyl 3-hydroxylation of clade A (type I, II and III) collagens and can lead to changes in lysine
340 post-translational modifications due to loss of its chaperone function[10, 11]. In this study, we found
341 that the mature collagen cross-links (HP residues per collagen) were markedly increased in the
342 FDL and Achilles tendons as well as the patellar ligament of *Crtap*$^{-/-}$ mice relative to wildtype.
343 Interestingly, we observed increased cross-links in the Achilles, but not FDL or patellar tendons
344 of 1-month old heterozygous mice, indicating a mild haploinsufficient effect of Crtap on this
345 tendon biochemical property. Outside of the genotype-specific effects, we saw an age-dependent

346 increase in HP residues per collagen in all genotypes. This observation is consistent with a study
347 by Taga and colleagues that reported an increase in 3-hydroxyproline residues in rat tendon
348 collagen (but not bone or skin) that plateaued at 3 months-of-age[31]. Taken together, these data
349 together with the TEM analyses suggest that altered collagen cross-linking in tendons and
350 ligaments from *Crtap*$^{-/-}$ mice may adversely affect collagen fibril assembly.

351 In addition to skeletal deformities and frequent fractures, severe OI is associated with
352 motor impairments including gait abnormalities, chronic pain and reduced muscle strength[8, 9, 32].
353 In this study, we showed that *Crtap*$^{-/-}$ mice exhibit reduced motor activity and coordination using
354 the open field, rotarod and grid footslip assays. We also observed a reduction in latency to fall on
355 the inverted grid assay that was mirrored by a dramatic loss of grip strength compared to
356 heterozygous and wildtype mice. These results are consistent with findings reported for the
357 *Col1a1*$^{Jrt/+}$ mouse model of severe OI and Ehlers-Danlos syndrome[17]. Specifically, Abdelaziz
358 and colleagues found that *Col1a1*$^{Jrt/+}$ mice displayed reduced motor activity using the open field
359 and running wheel assays – a phenotype they attributed to thermal hyperalgesia and mechanical
360 allodynia in these mice[33]. In this regard, the reduced vertical activity we observed in *Crtap*$^{-/-}$
361 mice may be indicative of a pain or spinal phenotype, suggesting that characterization of pain in
362 this model is a useful avenue for future research. Overall, this study represents one of the first
363 extensive characterizations of behavioral deficits in a mouse model of severe, recessive OI that
364 also correlates these deficits to tendon phenotypes.

365 Taken together, this study provides the first evidence for tendon and ligament phenotypes
366 in the *Crtap*$^{-/-}$ mouse model of severe recessive OI. We also provide compelling evidence for a
367 strong motor activity and coordination phenotype in these mice. As quality of life is so impacted
368 in patients with OI, a more comprehensive evaluation of behavioral outcomes in future

preclinical studies may provide important insights into the efficacy of therapeutic interventions.

392 **AUTHOR CONTRIBUTIONS**

393 M. W. Grol: Conception and design of the study, acquisition, analysis and interpretation of data,
394 drafting and editing of manuscript

395 N. A. Haelterman: Acquisition and analysis of data, editing of manuscript

396 E. Munivez: Acquisition of data

397 M. Archer: Acquisition and analysis of data

398 D. Hudson: Acquisition, analysis and interpretation of data, editing of manuscript

399 S. F. Tufa: Acquisition and analysis of data

400 D. R. Keene: Acquisition, analysis and interpretation of data, editing of manuscript

401 D. Eyre: Analysis and interpretation of data, editing of manuscript

402 B H. Lee: Conception and design of the study, interpretation of data, editing of manuscript

403

404 **Conflicts**

405 No conflicts of interest to report.

406

407 **Funding**

408 BCM Intellectual and Developmental Disabilities Research Center (HD024064) from the Eunice
409 Kennedy Shriver National Institute Of Child Health & Human Development, the BCM
410 Advanced Technology Cores with funding from the NIH (AI036211, CA125123, and
411 RR024574), the Rolanette and Berdon Lawrence Bone Disease Program of Texas, and the BCM
412 Center for Skeletal Medicine and Biology and the Pamela and David Ott Center for Heritable
413 Disorders of Connective Tissue, and PMR Foundation: ERF Matterson Grant

414

415 **REFERENCES**

416 1. Nourissat G, Berenbaum F, Duprez D. Tendon injury: from biology to tendon repair. Nat Rev
417 Rheumatol 2015; 11: 223-233.
418 2. Screen HR, Berk DE, Kadler KE, Ramirez F, Young MF. Tendon functional extracellular
419 matrix. J Orthop Res 2015; 33: 793-799.
420 3. Kannus P. Structure of the tendon connective tissue. Scand J Med Sci Sports 2000; 10: 312-
421 320.
422 4. Kalson NS, Lu Y, Taylor SH, Starborg T, Holmes DF, Kadler KE. A structure-based
423 extracellular matrix expansion mechanism of fibrous tissue growth. Elife 2015; 4.
424 5. Saito M, Marumo K. Collagen cross-links as a determinant of bone quality: a possible
425 explanation for bone fragility in aging, osteoporosis, and diabetes mellitus. Osteoporos Int
426 2010; 21: 195-214.
427 6. Alford AI, Kozloff KM, Hankenson KD. Extracellular matrix networks in bone remodeling.
428 Int J Biochem Cell Biol 2015; 65: 20-31.
429 7. Lim J, Grafe I, Alexander S, Lee B. Genetic causes and mechanisms of Osteogenesis
430 Imperfecta. Bone 2017; 102: 40-49.
431 8. Arponen H, Makitie O, Waltimo-Siren J. Association between joint hypermobility, scoliosis,
432 and cranial base anomalies in paediatric Osteogenesis imperfecta patients: a retrospective
433 cross-sectional study. BMC Musculoskelet Disord 2014; 15: 428.
434 9. Primorac D, Anticevic D, Barisic I, Hudetz D, Ivkovic A. Osteogenesis imperfecta--multi-
435 systemic and life-long disease that affects whole family. Coll Antropol 2014; 38: 767-772.
436 10. Hudson DM, Eyre DR. Collagen prolyl 3-hydroxylation: a major role for a minor post-
437 translational modification? Connect Tissue Res 2013; 54: 245-251.

438 11. Morello R, Bertin TK, Chen Y, Hicks J, Tonachini L, Monticone M, et al. CRTAP is
439 required for prolyl 3- hydroxylation and mutations cause recessive osteogenesis imperfecta.
440 Cell 2006; 127: 291-304.
441 12. Baldridge D, Schwarze U, Morello R, Lennington J, Bertin TK, Pace JM, et al. CRTAP and
442 LEPRE1 mutations in recessive osteogenesis imperfecta. Hum Mutat 2008; 29: 1435-1442.
443 13. Barnes AM, Chang W, Morello R, Cabral WA, Weis M, Eyre DR, et al. Deficiency of
444 cartilage-associated protein in recessive lethal osteogenesis imperfecta. N Engl J Med 2006;
445 355: 2757-2764.
446 14. Cabral WA, Chang W, Barnes AM, Weis M, Scott MA, Leikin S, et al. Prolyl 3-hydroxylase
447 1 deficiency causes a recessive metabolic bone disorder resembling lethal/severe
448 osteogenesis imperfecta. Nat Genet 2007; 39: 359-365.
449 15. van Dijk FS, Nesbitt IM, Zwikstra EH, Nikkels PG, Piersma SR, Fratantoni SA, et al. PPIB
450 mutations cause severe osteogenesis imperfecta. Am J Hum Genet 2009; 85: 521-527.
451 16. Baldridge D, Lennington J, Weis M, Homan EP, Jiang MM, Munivez E, et al. Generalized
452 connective tissue disease in *Crtap*$^{-/-}$ mouse. PLoS One 2010; 5: e10560.
453 17. Chen F, Guo R, Itoh S, Moreno L, Rosenthal E, Zappitelli T, et al. First mouse model for
454 combined osteogenesis imperfecta and Ehlers-Danlos syndrome. J Bone Miner Res 2014; 29:
455 1412-1423.
456 18. Terajima M, Taga Y, Chen Y, Cabral WA, Hou-Fu G, Srisawasdi S, et al. Cyclophilin-B
457 modulates collagen cross-linking by differentially affecting lysine hydroxylation in the
458 helical and telopeptidyl domains of tendon type I collagen. J Biol Chem 2016; 291: 9501-
459 9512.

460 19. Vranka JA, Pokidysheva E, Hayashi L, Zientek K, Mizuno K, Ishikawa Y, et al. Prolyl 3-
461 hydroxylase 1 null mice display abnormalities in fibrillar collagen-rich tissues such as
462 tendons, skin, and bones. J Biol Chem 2010; 285: 17253-17262.
463 20. Nixon AJ, Grol MW, Lang HM, Ruan MZC, Stone A, Begum L, et al. Disease-modifying
464 osteoarthritis treatment with interleukin-1 receptor antagonist gene therapy in small and large
465 animal models. Arthritis Rheumatol 2018; 70: 1757-1768.
466 21. Ruan MZ, Dawson B, Jiang MM, Gannon F, Heggeness M, Lee BH. Quantitative imaging of
467 murine osteoarthritic cartilage by phase-contrast micro-computed tomography. Arthritis
468 Rheum 2013; 65: 388-396.
469 22. Ruan MZ, Erez A, Guse K, Dawson B, Bertin T, Chen Y, et al. Proteoglycan 4 expression
470 protects against the development of osteoarthritis. Sci Transl Med 2013; 5: 176ra134.
471 23. Stone A, Grol MW, Ruan MZC, Dawson B, Chen Y, Jiang MM, et al. Combinatorial *Prg4*
472 and *Il-1ra* gene therapy protects against hyperalgesia and cartilage degeneration in post-
473 traumatic osteoarthritis. Hum Gene Ther 2019; 30: 225-235.
474 24. Schindelin J, Arganda-Carreras I, Frise E, Kaynig V, Longair M, Pietzsch T, et al. Fiji: an
475 open-source platform for biological-image analysis. Nat Methods 2012; 9: 676-682.
476 25. Eyre D. Collagen cross-linking amino acids. Methods Enzymol 1987; 144: 115-139.
477 26. Hudson DM, Archer M, King KB, Eyre DR. Glycation of type I collagen selectively targets
478 the same helical domain lysine sites as lysyl oxidase-mediated cross-linking. J Biol Chem
479 2018; 293: 15620-15627.
480 27. Steinmann S, Pfeifer CG, Brochhausen C, Docheva D. Spectrum of tendon pathologies:
481 triggers, trails and end-state. Int J Mol Sci 2020; 21.

482 28. Grafe I, Yang T, Alexander S, Homan EP, Lietman C, Jiang MM, et al. Excessive
483 transforming growth factor-beta signaling is a common mechanism in osteogenesis
484 imperfecta. Nat Med 2014; 20: 670-675.
485 29. Lim J, Munivez E, Jiang MM, Song IW, Gannon F, Keene DR, et al. mTORC1 signaling is a
486 critical regulator of postnatal tendon development. Sci Rep 2017; 7: 17175.
487 30. Bateman JF, Boot-Handford RP, Lamande SR. Genetic diseases of connective tissues:
488 cellular and extracellular effects of ECM mutations. Nat Rev Genet 2009; 10: 173-183.
489 31. Taga Y, Kusubata M, Ogawa-Goto K, Hattori S. Developmental stage-dependent regulation
490 of prolyl 3-hydroxylation in tendon type I collagen. J Biol Chem 2016; 291: 837-847.
491 32. Garman CR, Graf A, Krzak J, Caudill A, Smith P, Harris G. Gait deviations in children with
492 Osteogenesis Imperfecta Type I. J Pediatr Orthop 2019; 39: e641-e646.
493 33. Abdelaziz DM, Abdullah S, Magnussen C, Ribeiro-da-Silva A, Komarova SV, Rauch F, et
494 al. Behavioral signs of pain and functional impairment in a mouse model of osteogenesis
495 imperfecta. Bone 2015; 81: 400-406.

496
497
498
499
500
501
502
503
504

505 **FIGURE LEGENDS**

506 Figure 1. **Loss of Crtap causes thinning and hypercellularity of tendons and ligaments in**
507 **young and mature mice.** A-C, representative H&E images of 1-month ankle joints. D-F,
508 representative H&E images of 1-month knee joints. G-I, representative H&E images of 4-month
509 ankle joints. J-L, representative H&E images of 4-month knee joints. For all micrographs, higher
510 magnification images of the myotendinous junction (bottom-left), mid-tendon (bottom-center)
511 and insertion (bottom-right) are illustrated. n = 3-4 mice per group. Scale bar is 1 mm. M,
512 representative phase-contrast μCT images of 4-month wildtype (left) and *Crtap*$^{-/-}$ (right) knee
513 joints. Blue indicates the patellar ligament, green indicates the femoral articular cartilage, and red
514 indicates the tibial articular cartilage. Scale bar is 1 mm. N, volumetric quantification of the
515 patellar ligament volume in wildtype, heterozygous and *Crtap*$^{-/-}$ mice. * indicates $p < 0.05$. n = 3
516 mice per group.

517

518 Figure 2. **Collagen fibril diameter is altered in tendons and ligaments from heterozygous**
519 **and *Crtap*$^{-/-}$ mice.** A-C, representative TEM images of 4-month FDL tendon collagen fibrils.
520 Scale bar is 500 nm. D, representative histogram of size distribution for collagen fibrils in FDL
521 tendons. Data are representative of n = 3 mice. E-G, representative TEM images of 4-month
522 Achilles tendon collagen fibrils. Scale bar is 500 nm. H, representative histogram of size
523 distribution for collagen fibrils in Achilles tendons. Data are representative of n = 3 mice. E-G,
524 representative TEM images of 4-month patellar ligament collagen fibrils. Scale bar is 500 nm. H,
525 representative histogram of size distribution for collagen fibrils in patellar ligaments. Data are
526 representative of n = 3 mice per group.

527

528 Figure 3. **Collagen cross-linking is increased in tendons and ligaments from young and**
529 **mature *Crtap*$^{-/-}$ mice.** Quantification of collagen cross-links as hydroxylysyl-pyridinoline (HP)
530 residues per collagen for: A, FDL tendons; B, Achilles tendons; and C, patellar ligaments. Data
531 are means ± S.D. * indicates $p < 0.05$. n = 3-4 mice per group.
532
533 Figure 4. **Motor activity and coordination is impaired in 4-month-old *Crtap*$^{-/-}$ mice.** A-B,
534 quantification of spontaneous motor activity including (A) horizontal and (B) vertical activity
535 over a 30-min period using the open field assay. Data are min-to-max box and whisker plots with
536 individual points indicated. C, quantification of motor activity, coordination and endurance
537 across 10 trials conducted over 2 days using an accelerating rotarod assay. Data are means ± S.D.
538 Black asterisks indicates $p < 0.05$ compared to wildtype mice, and blue asterisks indicates $p <$
539 0.05 compared to heterozygous mice. D-E, quantification of (D) forelimb and (E) hindlimb
540 motor coordination using the grid footslip assay. Data are min-to-max box and whisker plots
541 with individual points indicated. F, quantification of forelimb and hindlimb grip strength using
542 the inverted grid assay conducted for 120 s. A reduction in the latency to fall indicates a reduced
543 grip strength. Data are min-to-max box and whisker plots with individual points indicated. G,
544 quantification of forelimb grip strength in N of force measured over 3 trials and then averaged.
545 Data are min-to-max box and whisker plots with individual points indicated. For all experiments,
546 * indicates $p < 0.05$. n = 9-12 mice per group.

FIGURE 1

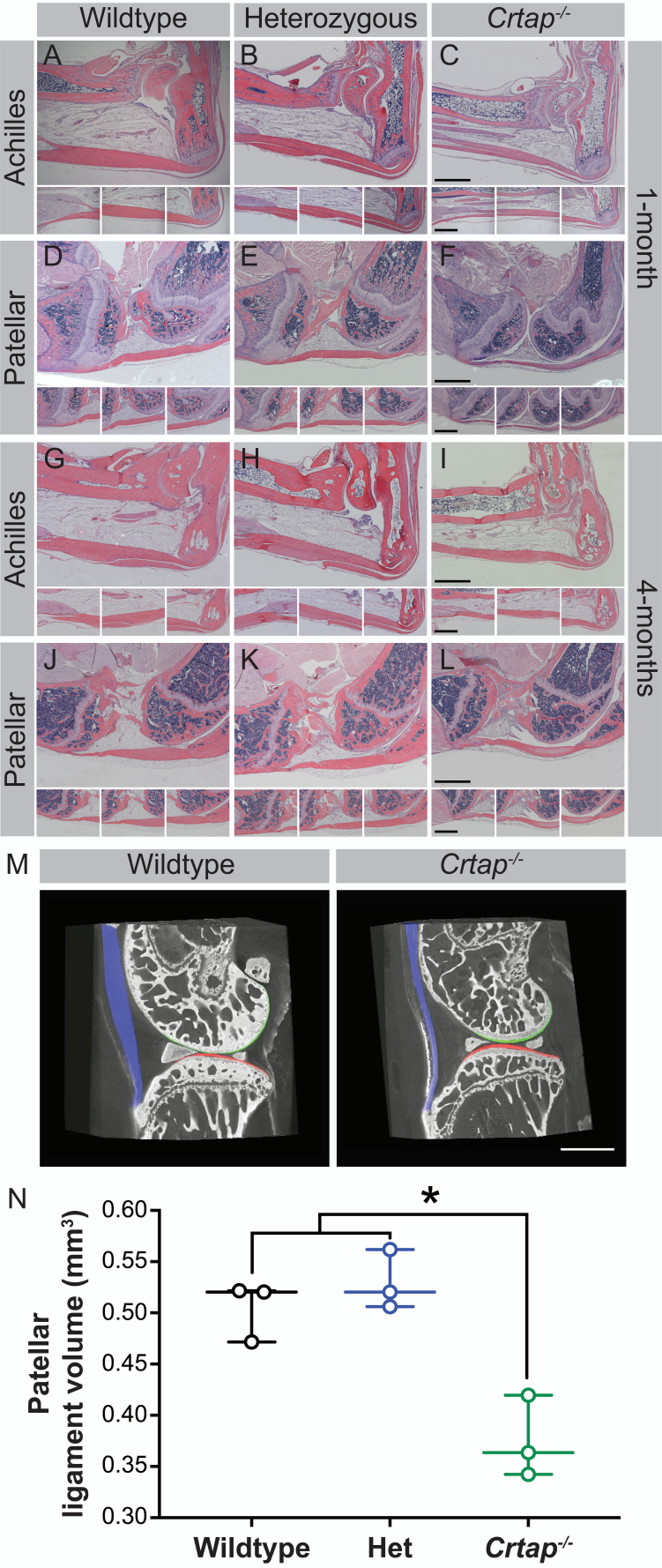
Wildtype
Heterozygous
Crtap-/-
Achilles
Patellar
1-month
4-months
A
B
C
D
E
F
G
H
I
J
K
L
M
N
Wildtype
Crtap-/-
*
Patellar ligament volume (mm3)
0.60
0.55
0.50
0.45
0.40
0.35
0.30
Wildtype
Het
Crtap-/-

FIGURE 2

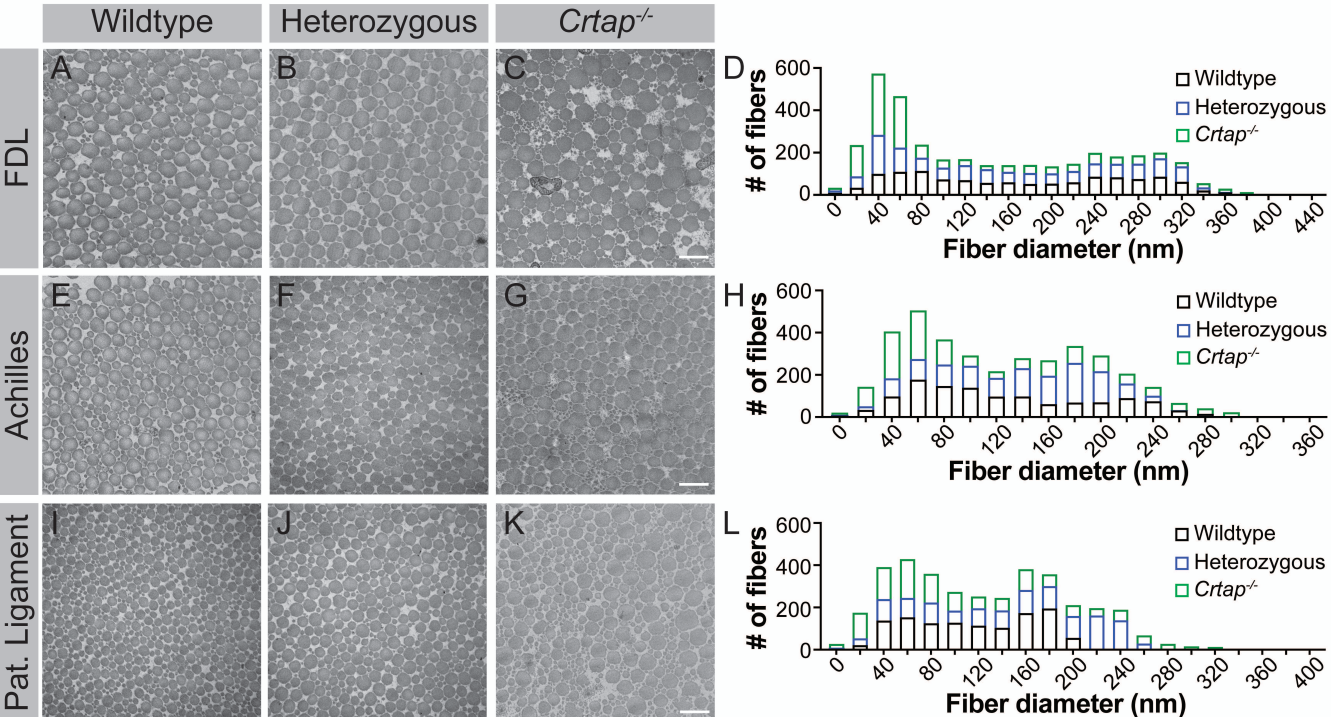
Wildtype
Heterozygous
Crtap-/-
FDL
Achilles
Pat. Ligament
A
B
C
D
E
F
G
H
I
J
K
L
# of fibers
Fiber diameter (nm)
Wildtype
Heterozygous
Crtap-/-

FIGURE 3

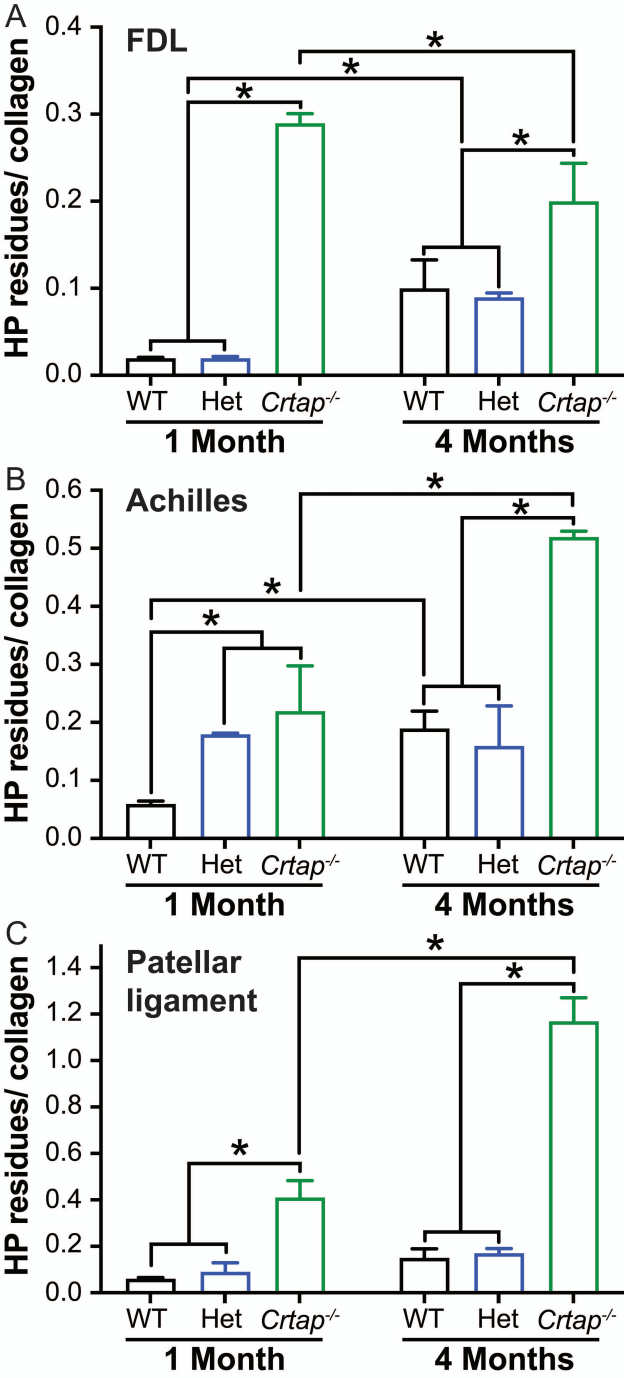
A
FDL
HP residues/ collagen
0.4
0.3
0.2
0.1
0.0
*
*
*
*
WT
Het
Crtap-/-
WT
Het
Crtap-/-
1 Month
4 Months
B
Achilles
HP residues/ collagen
0.6
0.5
0.4
0.3
0.2
0.1
0.0
*
*
*
*
WT
Het
Crtap-/-
WT
Het
Crtap-/-
1 Month
4 Months
C
Patellar ligament
HP residues/ collagen
1.4
1.2
1.0
0.8
0.6
0.4
0.2
0.0
*
*
*
WT
Het
Crtap-/-
WT
Het
Crtap-/-
1 Month
4 Months

FIGURE 4

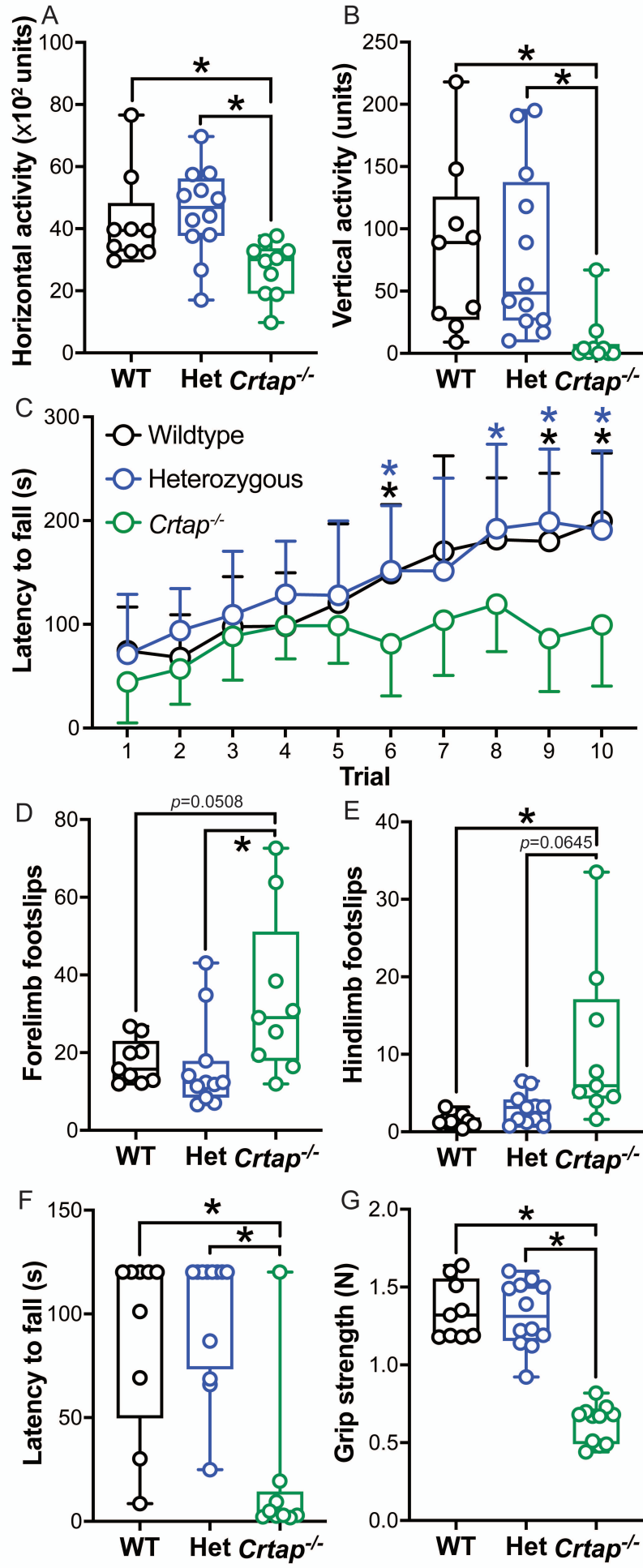
A
Horizontal activity (x10² units)
100
80
60
40
20
0
*
*
WT
Het
Crtap-/-
B
Vertical activity (units)
250
200
150
100
50
0
*
*
WT
Het
Crtap-/-
C
Latency to fall (s)
300
200
100
0
Wildtype
Heterozygous
Crtap-/-
1
2
3
4
5
6
7
8
9
10
Trial
D
Forelimb footslips
80
60
40
20
0
p=0.0508
*
WT
Het
Crtap-/-
E
Hindlimb footslips
40
30
20
10
0
*
p=0.0645
WT
Het
Crtap-/-
F
Latency to fall (s)
150
100
50
0
*
*
WT
Het
Crtap-/-
G
Grip strength (N)
2.0
1.5
1.0
0.5
0.0
*
*
WT
Het
Crtap-/-